

CHARACTERIZATION OF ABANDONED ROCKET BODY FAMILIES FOR ACTIVE REMOVAL

Carmen Pardini

ISTI – Consiglio Nazionale delle Ricerche (CNR), Pisa, Italy, Carmen.Pardini@isti.cnr.it

Luciano Anselmo

ISTI – Consiglio Nazionale delle Ricerche (CNR), Pisa, Italy, Luciano.Anselmo@isti.cnr.it

A new ranking index was developed and applied to a wide set of rocket body families, characterized by stage dry masses greater than 500 kg and by the presence of at least 5 stages abandoned in LEO. The upper stages selected accounted for more than 80% of the unclassified rocket bodies in LEO and nearly 95% of the associated dry mass. The detailed results obtained for 657 objects clearly identified the most critical altitude-inclination bands and stage models, to be targeted first if and when a debris remediation strategy including the active removal of intact abandoned objects were deemed necessary. Apart from the evaluation of the criticality regarding the long-term evolution of the debris environment, resulting in a priority listing for optimal active removal, the application of the new ranking index is not limited to debris remediation. In fact, if applied before launch to spacecraft and rocket bodies to be disposed in orbit, at the end of mission, it would provide an additional debris mitigation analysis tool for evaluating competing disposal options. Concerning the rocket bodies abandoned in LEO, 274 resulted to have a criticality equal or larger than the average intact object abandoned in an 800 km sun-synchronous orbit. Among them, 243 belonged to the Russian Federation and Ukraine, 25 to China, 5 to Europe and 1 to Japan. In addition to being concentrated in relatively few and narrow altitude-inclinations bands, the most numerous rocket body families often present a quite uniform distribution in right ascension of the ascending node, which is especially convenient for multiple target removal missions.

Keywords: Space Debris, Environmental Criticality, Ranking Index, Active Removal, Geopolitical Distribution, Abandoned Rocket Bodies in LEO.

I. INTRODUCTION

Most of the cross-sectional area and mass in orbit are concentrated in intact objects, of which approximately 80% are constituted by abandoned spacecraft and rocket bodies. In Low Earth Orbit (LEO), the abandoned objects and the associated mass are not evenly distributed, but quite often concentrated in relatively narrow altitude-inclination bands (see Figures 1 and 2), where the probability of catastrophic collision is significantly above the average. (The expected total collision rate in LEO among cataloged objects is currently around 0.2 per year, about 30% of which involving collisions among intact bodies [1].

This clustering pattern frequently involves a substantial number of nearly identical objects, as upper stages of a few basic models. Therefore, even though upper stages account for about 50% of the abandoned mass in LEO, such a 50% is concentrated in a relatively small number of rocket body families [2]. It seems then quite reasonable that any plausible orbital debris remediation scheme, if and when deemed necessary, should start considering the active removal of abandoned mass from crowded regions, and the targeting of upper stages in particular would offer a lot of advantages, because they are usually easier and safer to grab, more robust from a structural point of view, less secretive, and have simpler and more symmetrical shapes, mass distributions, structures and rotational motions [3] [4] [5]. In addition, the targeting of very similar objects belonging to a few types would make possible many removal missions with basically the same hardware and procedures [6].

This paper characterizes the most relevant rocket body families present in LEO in terms of mass, orbit, residual lifetime and catastrophic debris collision probability. Just 9 general types of rocket bodies, contributing with at least 20 metric tons to the mass in LEO at the end of 2015, account for nearly 73% of the stages and nearly 86% of the overall mass stored in upper stages abandoned below the average altitude of 2000 km. Through the definition of a simplified ranking scheme based on reasonable and easy to apply assumptions, the results obtained are used to evaluate and prioritize the most relevant families of objects, and the single objects belonging to each family, in order to find the most appropriate potential targets for active debris removal as a function of mass to be de-orbited, average

altitude, inclination and node distribution (being the latter information of relevance for multiple removal approaches). The details provided aim to be useful for active removal mission preliminary design, dimensioning and analysis.

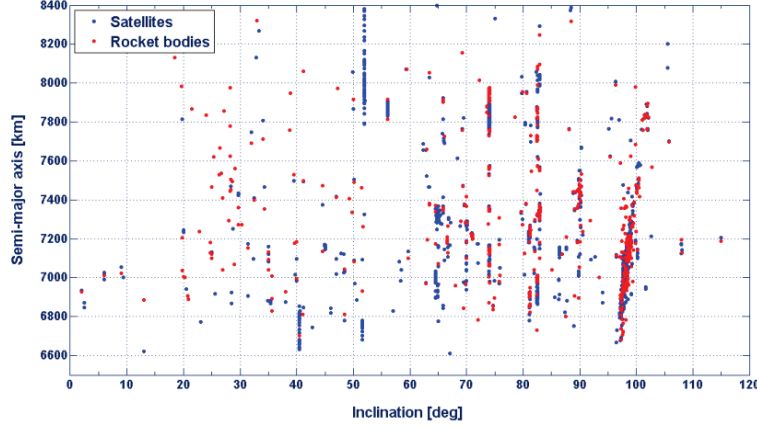


Fig. 1: Distribution of intact satellites and rocket bodies fully residing in LEO as a function of semi-major axis and inclination (November 25, 2015). The Earth's equatorial radius is about 6378 km.

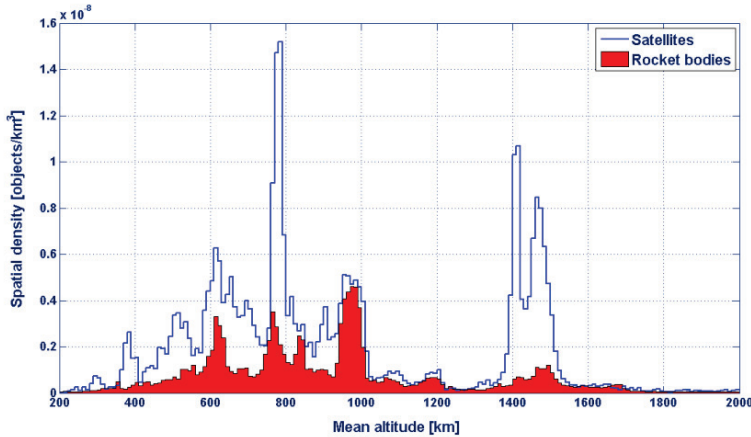


Fig. 2: Spatial density in LEO of intact satellites and rocket bodies (November 25, 2015).

II. ROCKET BODIES IN ORBIT

Detailed information on the unclassified rocket bodies in orbit at the beginning of 2015 was provided elsewhere [2]. Herein, the outcomes of a more recent census, showing a snapshot of the situation about ten months afterwards (25 November 2015), are presented. Among 1694 upper stages for which a state vector was available, 811, i.e. approximately 48%, had a mean altitude ≤ 2000 km. The estimated total mass was 2778 metric tons, of which 1196 metric tons, i.e. about 43%, in LEO. The average rocket body mass was 1609 kg; for the upper stages with a mean altitude ≤ 2000 km, the average mass was 1460 kg. Figures 3 and 4 detail the geopolitical distribution of the upper stages in terms of number and mass, respectively. The situation in LEO is further expanded in Figures 5 and 6.

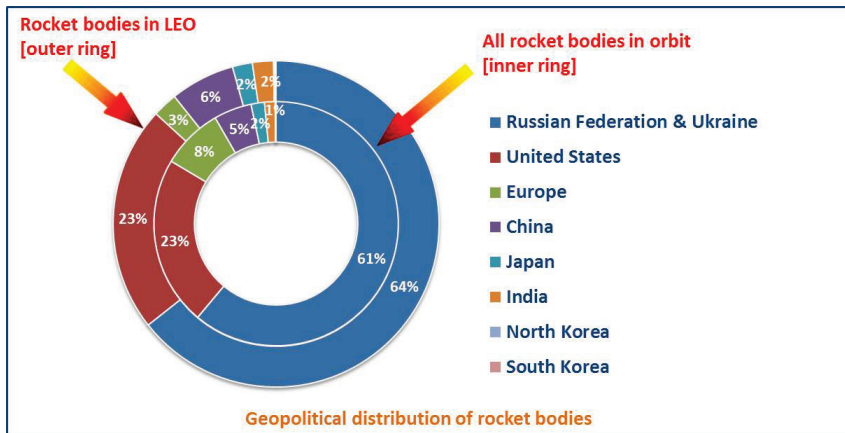


Fig. 3: Percentage geopolitical distribution of rocket bodies with unclassified orbits (November 25, 2015).

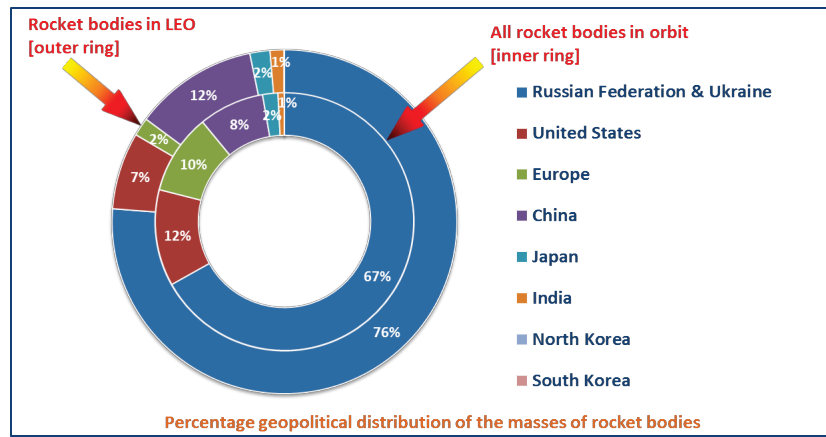


Fig. 4: Percentage geopolitical distribution of the mass of rocket bodies with unclassified orbits (November 25, 2015).

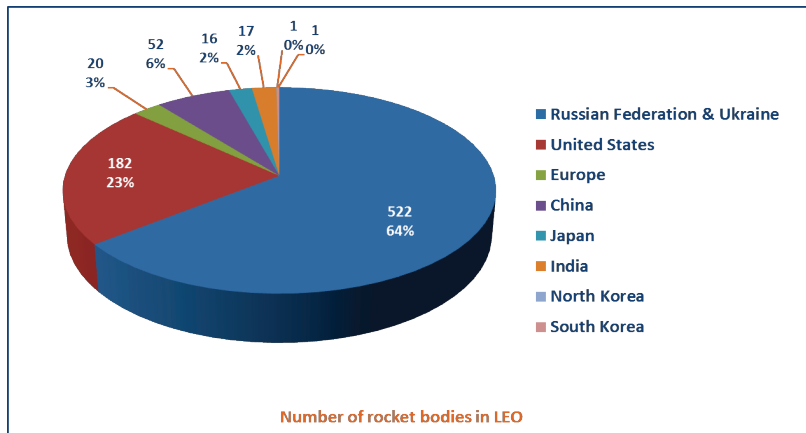


Fig. 5: Geopolitical distribution of rocket bodies in LEO with unclassified orbits (November 25, 2015).

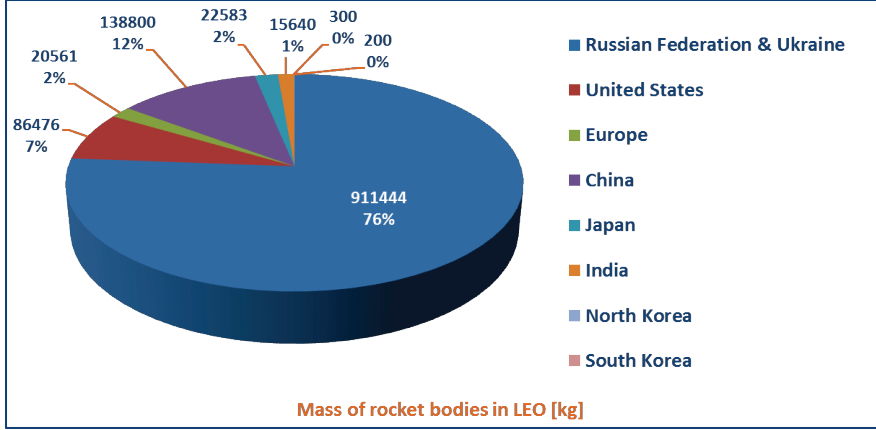


Fig. 6: Geopolitical distribution of the mass of rocket bodies in LEO with unclassified orbits (November 25, 2015).

In terms of upper stages mass abandoned in orbit around the Earth, the Russian Federation and Ukraine, taken together, account for 67% of the total, the United States for 12%, Europe for 10%, China for 8%, Japan for 2% and India for 1% (Figure 4). Focusing the attention in LEO, the Russian Federation and Ukraine lead is still more prominent, with 76% of the total, followed by China with 12%, the United States with 7%, Japan and Europe with 2%, and India with 1% (Figures 4 and 6).

Concerning the types, dry masses and orbital distributions of the unclassified upper stages present in orbit on 25 November 2015, further details are provided in Figures 7 and 8 for the Russian Federation and Ukraine, in Figures 9 and 10 for Europe, in Figures 11 and 12 for China, in Figures 13 and 14 for Japan, and in Figures 15 and 16 for the United States. Regarding India, 23 out of 24 rocket bodies in orbit, of which 16 out of 17 in LEO, were fourth stages of the PSLV launcher, with a dry mass of 920 kg.

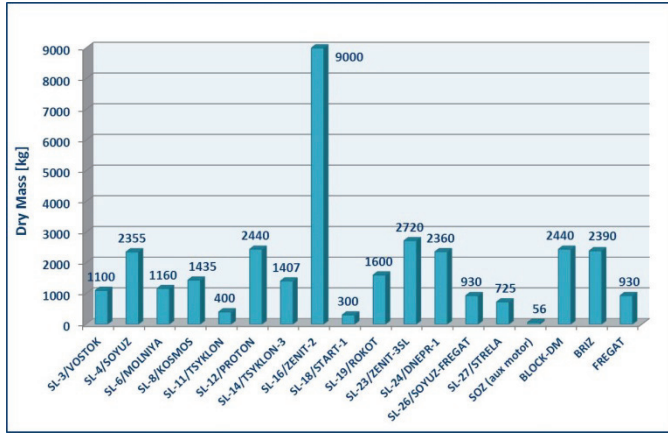


Fig. 7: Dry masses of the upper stages launched by the Russian Federation and Ukraine [2].

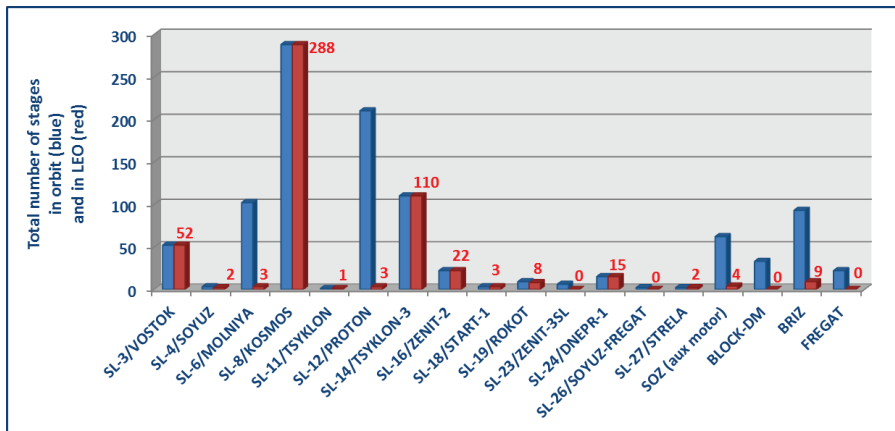


Fig. 8: Distribution among rocket types and orbital regimes of the upper stages launched by the Russian Federation and Ukraine.

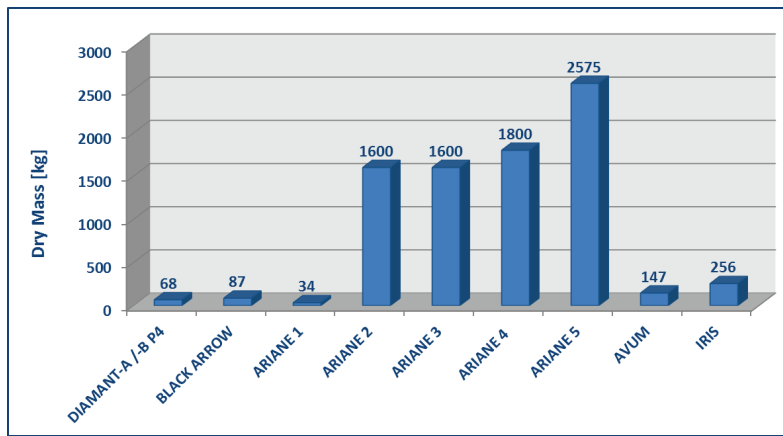


Fig. 9: Dry masses of the upper stages launched by Europe [2].

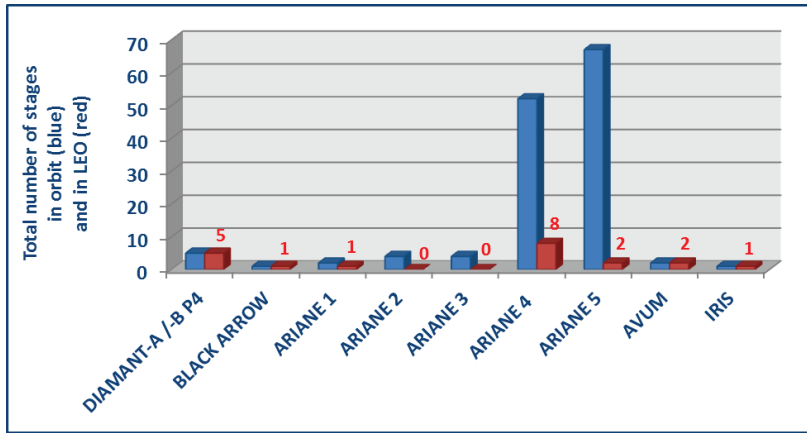


Fig. 10: Distribution among rocket types and orbital regimes of the upper stages launched by Europe.

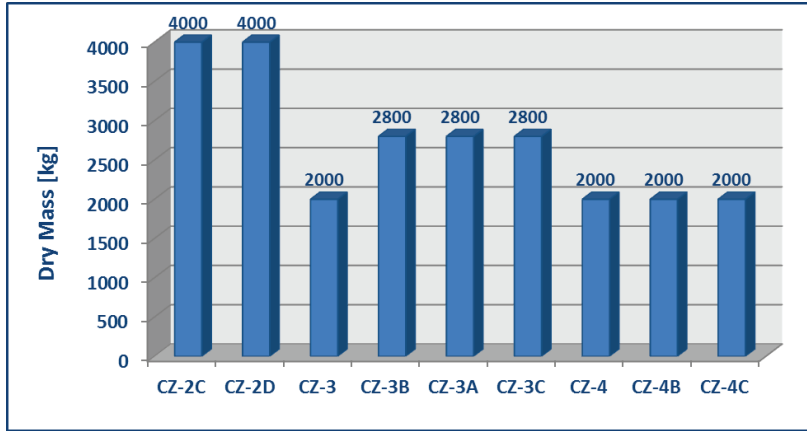


Fig. 11: Dry masses of the upper stages launched by China [2].

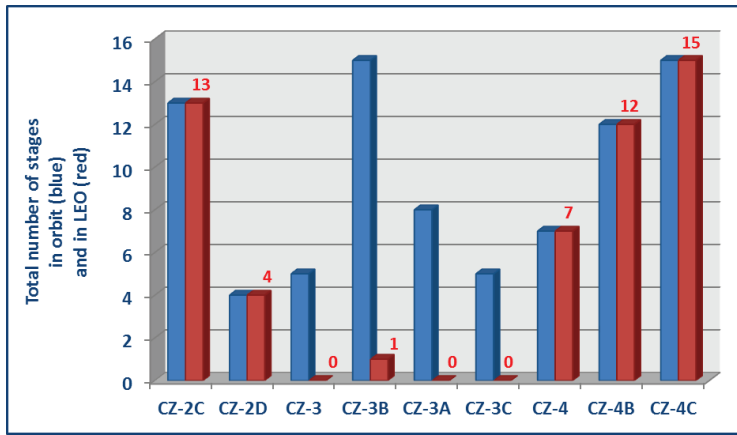


Fig. 12: Distribution among rocket types and orbital regimes of the upper stages launched by China.

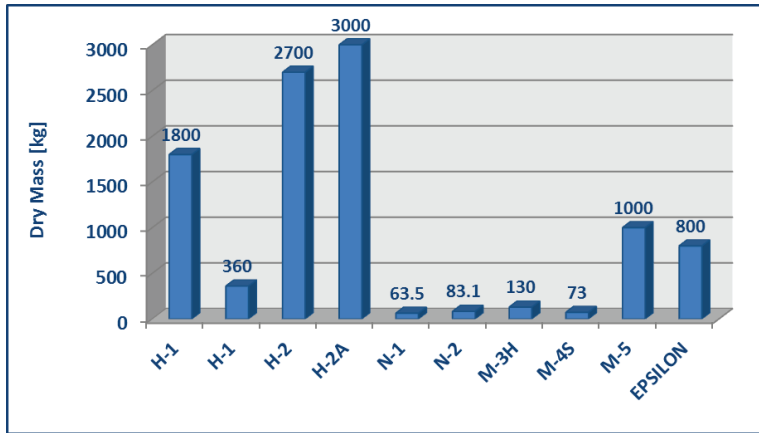


Fig. 13: Dry masses of the upper stages launched by Japan [2].

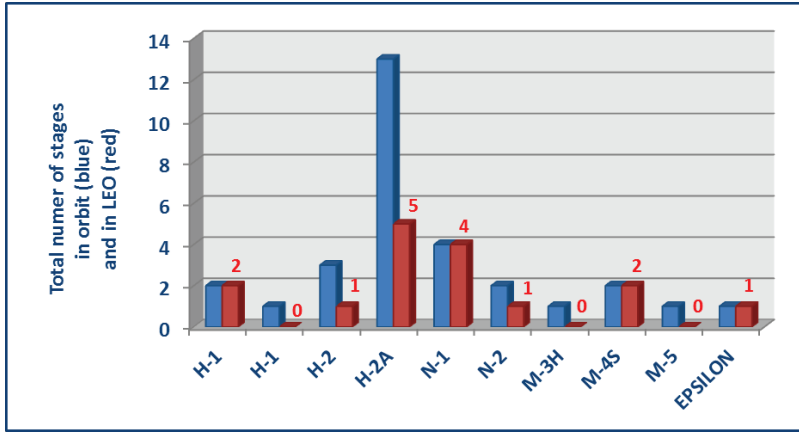


Fig. 14: Distribution among rocket types and orbital regimes of the upper stages launched by Japan.

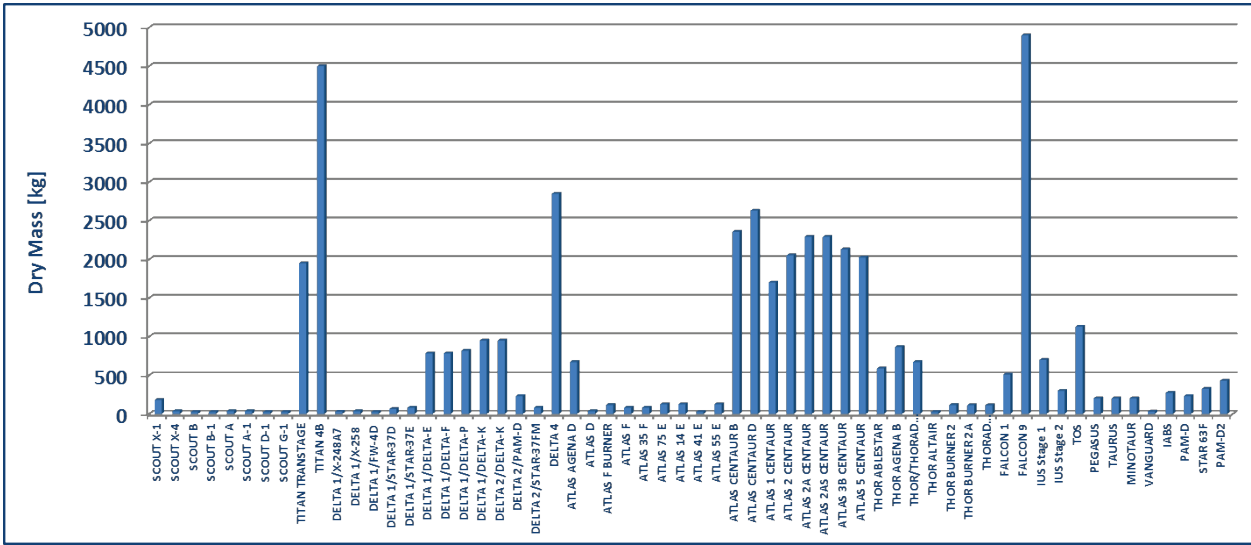


Fig. 15: Dry masses of the upper stages launched by the United States [2].

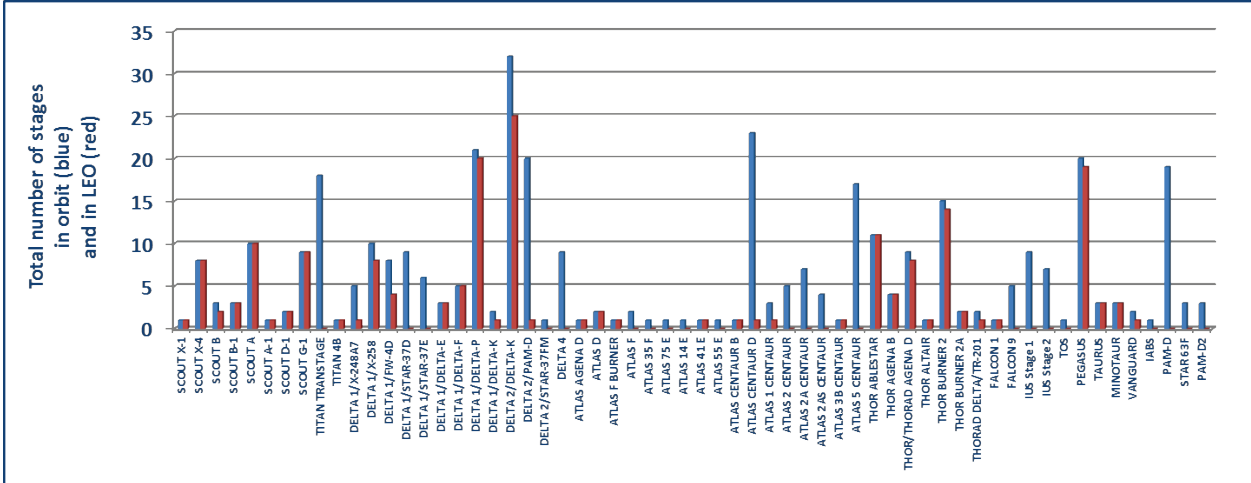


Fig. 16: Distribution among rocket types and orbital regimes of the upper stages launched by the United States.

III. ROCKET BODIES IN LEO CONSIDERED IN THE RANKING ANALYSIS

In this paper, the rocket body families analyzed were those characterized by a stage dry mass > 500 kg and by the presence of ≥ 5 stages abandoned in LEO. They are listed in Table 1 and represented more than 80% of the unclassified rocket bodies in LEO (657 out of 811) and nearly 95% of the associated dry mass (1132 out of 1199 metric tons), as of November 25, 2015. The corresponding geopolitical distribution, in terms of mass, is summarized in Figure 17. Nearly 79% of the ranked rocket body mass belonged to the Russian Federation and Ukraine, 12% to China, 5% to the United States, and the remaining 4% to Japan, Europe and India.

ROCKET BODY	DRY MASS [kg]	STAGE	NUMBER OF STAGES IN LEO	TOTAL MASS OF THE STAGES IN LEO [kg]
RUSSIAN FEDERATION & UKRAINE				
SL-3 VOSTOK	1100	Stage 2 Vostok 8A92-M-2	52	57,200
SL-8 KOSMOS	1435	Stage 2 2 Kosmos-1 & 288 Kosmos-3M 11K65M	288	413,280
SL-14 TSYKLON-3	1407	Stage 3 Tsyklon-3	110	154,770
SL-16 ZENIT-2	9000	Stage 2 Zenit-2	22	198,000
SL-19 ROKOT	1600	Stage 3 Rokot-3 Briz	8	12,800
SL-24 DNEPR-1	2360	Stage 3 Dnepr	15	35,400
BRIZ	2390	Briz-M upper stage	9	21,510
TOTAL NUMBER AND MASS			504	892,960
EUROPE				
ARIANE 40 & 42P	1800	Stage 3 H10	8	14,400
UNITED STATES				
DELTA 1	785 (DELTA-E) 784 (DELTA-F) 820 (DELTA-P) 950 (DELTA-K)	Stage 2 3 DELTA-E 5 DELTA-F 20 DELTA-P 1 DELTA-K	29	23,625
DELTA 2	950	Stage 2 DELTA-K	25	23,750
THOR ABLESTAR	590	Stage 2 Able-Star	11	6490
THOR & THORAD AGENA D	673	Stage 2 Agena-D	8 (5 THOR & 3 THORAD)	5384
TOTAL NUMBER AND MASS			73	59,249
CHINA				
CZ-2C	4000	Stage 2	13	52,000
CZ-2D	4000	Stage 2	4	16,000
CZ-4	2000	Stage 3	7	14,000
CZ-4B	2000	Stage 3	12	24,000
CZ-4C	2000	Stage 3	15	30,000
TOTAL NUMBER AND MASS			51	136,000
JAPAN				
H-2A	3000	Stage 2	5	15,000
INDIA				
PSLV	920	Stage 4	16	14,720
OVERALL NUMBER AND MASS IN LEO			657	1,132,329

Table 1: Rocket bodies in LEO considered in the ranking analysis.

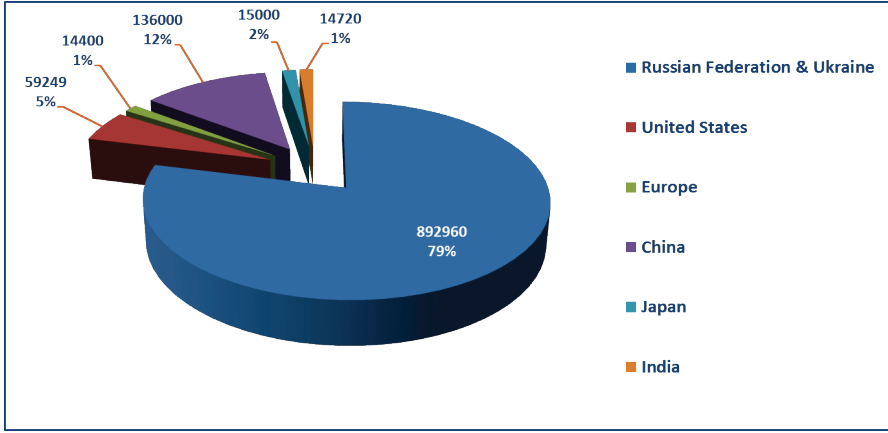


Fig. 17: Geopolitical distribution of the mass of the rocket bodies in LEO considered in the ranking analysis. The mass taken into account represented nearly 95% of the total.

IV. RANKING UPPER STAGES FOR ENVIRONMENTAL CRITICALITY AND ACTIVE REMOVAL

In recent years, a growing popular way to evaluate the latent long-term environmental impact of orbiting objects, avoiding thousands of complex simulations based on quite uncertain assumptions, was the recourse to ranking schemes based on reasonable hypotheses and simplifications [4] [7] [8] [9] [10] [11] [12] [13] [14] [15]. In this study, the task of ranking a broad and representative selection of rocket bodies in LEO, with the goal of evaluating their potential detrimental effects on the debris environment and the relative benefit of having them actively deorbited, was tackled by applying a new ranking scheme, introduced in a recent paper [2], further developing and simplifying an approach elaborated by the authors during the last few years [4] [11] [14].

In principle, the proposed ranking index could be used for any object in LEO (abandoned spacecraft included) and would be able to sort out the targets potentially most critical for the future preservation of the LEO protected region [16], but its application to rocket bodies, i.e. to a few relatively homogeneous families of objects, is much more straightforward, reliable and meaningful, as will result clear in the following, after the presentation of the index and the discussion of the results obtained.

IV.I Ranking Index Definition

In order to characterize the potential long-term adverse effects, on the LEO debris environment, of an abandoned object, the associated criticality ranking index R , where a higher index value is associated with a higher potential threat, should be proportional to the probability of catastrophic breakup P_c due to space debris collision during the object's orbital lifetime, to the number of new "effective projectiles" N_p possibly resulting from a breakup, and to the environmental impact over the long-term of the consequent debris cloud [11] [14].

Being $F(t)$ the flux of orbital debris able to significantly breakup a target intact object, A the average collisional cross-section of the latter, L_T its residual lifetime in orbit and t the time, the probability of target fragmentation can be approximated by the following relationship, taking into account that $P_c < 0.1$ and that the cross-section of typical debris impactors is 2–4 orders of magnitude smaller than A for intact objects:

$$P_c \approx \int_0^{L_T} F(t) \cdot A \cdot dt. \quad (1)$$

Taking into account that the time evolution of $F(t)$ is affected by significant uncertainties [17] and that the estimate of the integral in Eq. (1) for each specific target object would be cumbersome, it was chosen to include in the ranking scheme just the current flux F_{cat} of catalogued debris, in order to maintain the index as simple and manageable as possible. It was then feasible to streamline Eq. (1) as follows:

$$P_c \sim F_{cat} \cdot A \cdot L_T, \quad (2)$$

which, for nearly circular orbits, the large majority in LEO, can be expressed as:

$$L_T \cong l(h) \cdot \frac{M}{A}, \quad (3)$$

being M/A the body mass-to-area ratio, h its mean altitude and $l(h)$ a “normalized” average lifetime function [11] [14], which was estimated for the average intact object in LEO in 2013 [1] [4], with $M_0 = 934$ kg and $A_0 = 11$ m², i.e. $A_0/M_0 = 0.012$ m²/kg. Eq. (2) then becomes:

$$P_c \sim F_{cat} \cdot l(h) \cdot M. \quad (4)$$

Looking at the fragments potentially generated by a catastrophic breakup, their cumulative number N_p , larger than a given characteristic size, can be roughly estimated with the NASA standard breakup model [18] [19]. N_p is proportional to the cumulative mass of the target object and impacting debris, raised to the 0.75th power. However, the cumulative mass is often very close to the target mass, being the latter typically much larger (by 2-3 orders of magnitude in LEO) than the impactor’s one. As a result, $N_p \propto M^{0.75}$, leading to the following definition of the criticality ranking index R :

$$R \propto P_c \cdot N_p \propto P_c \cdot M^{0.75} \sim F_{cat} \cdot l(h) \cdot M^{1.75}. \quad (5)$$

Other factors to be possibly incorporated in Eq. (5) were previously investigated [11] [14], aiming at the characterization of the long-term impact on the environment of the resulting debris cloud, but the added complication, coupled with the inherent uncertainties and the generally limited numerical impact of such improvements, led to the choice of adopting, for the analysis presented in this paper, the definition given in Eq. (5) [2]. As a matter of fact, also because most of the intact objects and debris in LEO are characterized by medium or high orbital inclinations, and this is still truer for the rocket bodies listed in Table 1, Eq. (5) already incorporates most of the story regarding the potential criticality of the target objects analyzed in the present study.

IV.II Normalized and Dimensionless Ranking Index

Starting from Eq. (5) and adopting as measurement unit the above mentioned average intact object in LEO in 2013 [4], placed into a sun-synchronous orbit with a mean altitude $h_0 = 800$ km and with an associated inclination $i_0 = 98.5^\circ$, a normalized and dimensionless ranking index R_N can be defined as follows:

$$R_N \equiv \frac{F_{cat}}{F_{0cat}} \cdot \frac{l(h)}{l(h_0)} \cdot \left(\frac{M}{M_0} \right)^{1.75}, \quad (6)$$

where F_{0cat} is the flux of cataloged debris on the reference object and $l(h)/l(h_0) \equiv 1$ when $h > h_0$. The latter cut off, set at an orbital lifetime of approximately 200 years, was introduced to avoid weighting too much objects with very long residual lifetimes, much longer than any reasonable temporal horizon for the current modeling and technology projections. A smaller lifetime cut off, around 100 years, could have been just as appropriate, but the former choice was dictated by the fact that many of the current debris modeling projections are ran over two centuries. The flux of cataloged debris on each rocket body, as well as on the reference object, was estimated with the Space Debris Impact Risk Analysis Tool (SDIRAT) [20] [21] [22]. To account for a possible non-uniform distribution of the cataloged population, the flux on each target object was estimated by averaging the fluxes corresponding to different orientations of the orbit in the inertial space (Earth equatorial reference frame). This was in practice realized by varying the Right Ascension of the Ascending Node (RAAN) by 30° until a full revolution was completed. The flux to be used in Eq. (6) was therefore the average of twelve (i.e. 360°/30°) fluxes on the same orbit rotating in space.

As already emphasized in previous papers [2] [4] [11] [14], the intuitive meaning of a ranking index defined in this way is easy to grasp, being R_N referred to an average intact object in LEO placed in the most popular orbital regime, the sun-synchronous one. The index value found for a specific object should therefore proportionally weight its latent detrimental effects on the long-term debris environment compared with those of the reference body.

This was, in fact, the goal of the original index definition presented in previous studies [11] [14], where the debris flux considered in Eq. (2) and following was also a function of the intact target mass, in order to take into account

the fact that a catastrophic breakup would occur only above a certain specific energy threshold [1]. The adoption of the flux of cataloged objects, irrespective of the target mass, as done here for building a more simple and easier to manage index, would therefore have the effect of overestimating the ranking index of the objects more massive than the reference one ($M_0 = 934$ kg) and underestimating the index of the lesser massive bodies.

However, even for the most massive upper stages considered ($M = 9000$ kg), the expected overestimation for having used the cataloged debris flux in the ranking index definition would be less than a factor of 2 (i.e. < 0.3 in logarithmic terms), and for smaller masses the enhancing would rapidly decrease (to $< 50\%$ for 4000 kg, $< 20\%$ for 2000 kg, and $< 10\%$ for 1500 kg). Concerning the least massive upper stages analyzed ($M = 590$ kg), the expected underestimation would be $< 20\%$, (i.e. < 0.1 in logarithmic terms). If these numbers are compared with the intrinsic complexity and all the uncertainties underlying the current and future debris environment [17], including the concept itself of catastrophic collision [1], the simplified approach used in this paper seems reasonable and appropriate. Moreover, the relative ranking indexes among similar intact bodies, belonging to homogeneous classes of objects with nearly the same mass, as the families of upper stages analyzed in this paper, are not affected at all by the choice adopted. Any bias, if present, would only appear when comparing the ranking indexes of heterogeneous objects of quite different masses.

IV.III Logarithmic Ranking Index

Even though R_N has a quite straightforward meaning, its values may span a range of several orders of magnitude, so a logarithmic index R_{NL} might be often more practical for summarizing the results. It was defined in the following way:

$$R_{NL} \equiv \log_{10}(R_N) + 1. \quad (7)$$

This choice assures that $R_{NL} = R_N = 1$ for the reference body, and $R_{NL} \geq 0$ when $R_N \geq 0.1$, i.e. 1/10 of the ranking index for the reference body. In other words, the targets deserving more attention, from a debris remediation point of view, are characterized by R_{NL} around 1 or larger, having a current environment criticality around the average or greater. The old abandoned objects for which $R_{NL} < 0$, i.e. with $M < 250$ kg in a sun-synchronous orbit at 800 km, on the other hand, are not enough critical for the future evolution of the environment to merit a high removal priority.

It should be, however, emphasized, that these arguments apply to an optimized step-by-step remediation of the situation created in the past, assuming for future launches and missions the strict application of mitigation guidelines [16]. The latter, in order to prevent a further growth of massive “projectiles” leading to an increase of the collision probability, should avoid the long-term presence in LEO of any new uncontrolled object, either intact or sizable debris, even with $M < 250$ kg, where the acceptable “long-term presence” could be a few decades or even less.

V. ROCKET BODIES CRITICALITY IN LEO

The ranking scheme developed and presented in the previous sections was applied to the families of upper stages in LEO listed in Table 1 and described in Section III. As already pointed out, they accounted for more than 80% of the unclassified rocket bodies and nearly 95% of the associated dry mass, as of January 7, 2015. Figure 18 shows the average ranking index found for the upper stages of each launcher included in the analysis. The dominance of the second stage of the Zenit-2 launcher, with an average ranking index much greater than 10, is undisputed, even taking into account the caveats illustrated in Section IV.II, due to the combination of rocket body mass and disposal orbits. On the other hand, for all the other rocket body families, the distribution of average ranking indexes is relatively compressed, with two families (CZ-2 second stage, Dnepr-1 third stage) between 2 and 3, three families (Kosmos second stage, CZ-4 third stage and Ariane 4 third stage) between 1 and 2, four families (Vostok second stage, Rokot third stage, Briz-M upper stage and H-2A second stage) between 0.5 and 1, and 5 families below 0.5. This grouping is substantially confirmed even looking at the rocket bodies presenting the maximum ranking index in each launcher family (Figure 19).

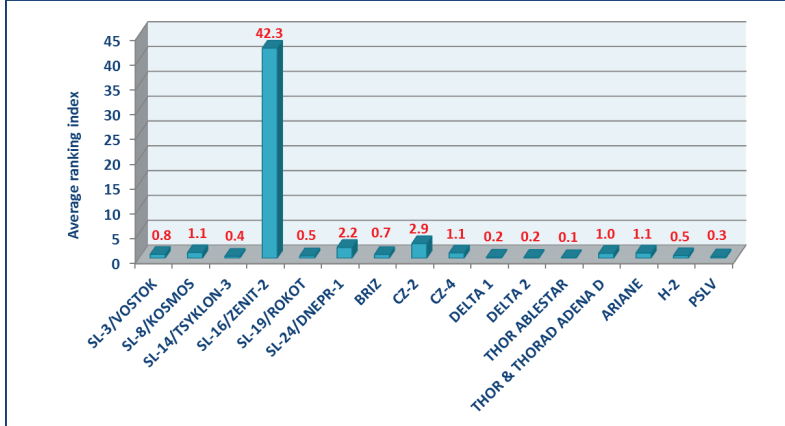


Fig. 18: Average ranking index found for each upper stage family associated with the listed launchers.

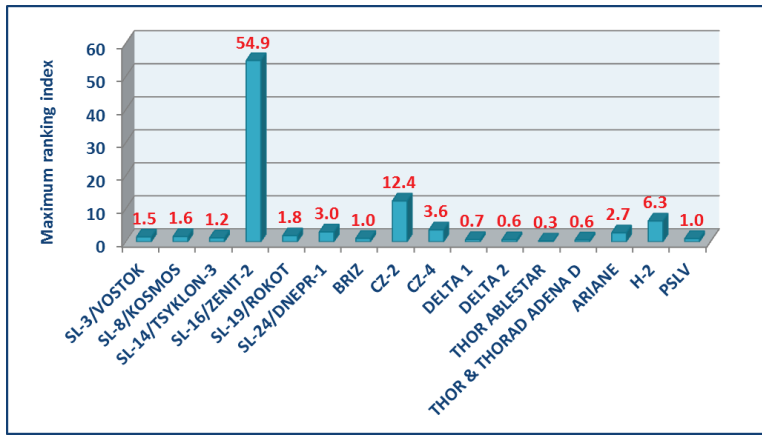


Fig. 19: Maximum ranking index found in each upper stage family associated with the listed launchers. The specific rocket bodies are identified by their catalog number.

However, the average and maximum values of the ranking index are not enough to have a clear picture of the situation in orbit, because how much a family is numerous is important as well, or even more. In fact, as shown in Figure 20, even though the Kosmos second stages have an average ranking index of 1.1, there are 162 of them with $R_N \geq 1$, followed by 30 Vostok second stages, 22 Zenit-2 second stages, 16 CZ-4 third stages, 14 Dnepr-1 third stages and 9 CZ-2 second stages. Looking at the rocket bodies with $R_N \geq 2$, following the 22 Zenit-2 second stages, there are 9 Dnepr-1 third stages, 8 CZ-4 third stages, 5 CZ-2 second stages and 4 Ariane 4 third stage.

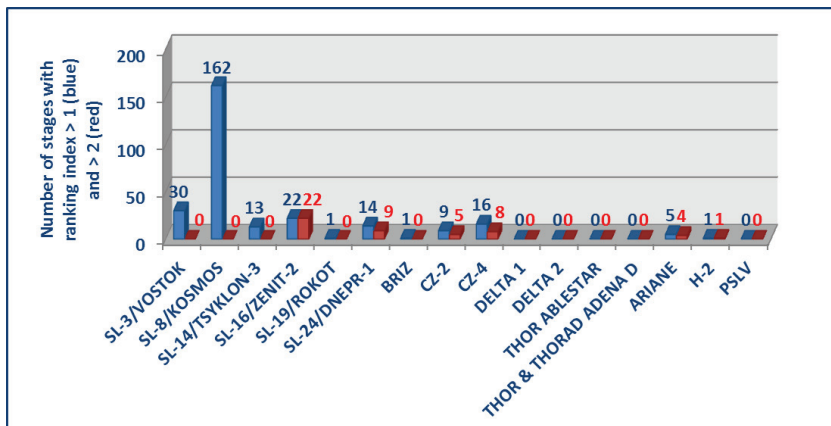


Fig. 20: Number of rocket bodies of each family, associated with the listed launchers, having a ranking index higher than 1 (blue) or 2 (red).

The detailed results obtained for the upper stages of the Russian and Ukrainian launchers are summarized in Figures 21 (orbital distribution), 22 (ranking index) and 23 (logarithmic ranking index). The rocket bodies are mostly grouped in a few and narrow inclination bands (Figure 21). Those for which $R_N \geq 0.1$ were found between 600 and 1800 km, and belonged to all the families (Figure 22). Those for which $R_N \geq 1$ were found between 600 and 1500 km, between 600 and 1100 km those for which $R_N \geq 2$.

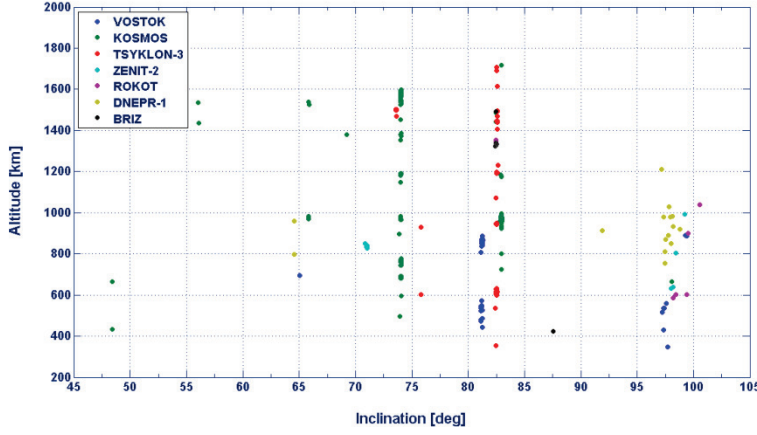


Fig. 21: Orbital distribution of the Russian and Ukrainian rocket bodies.

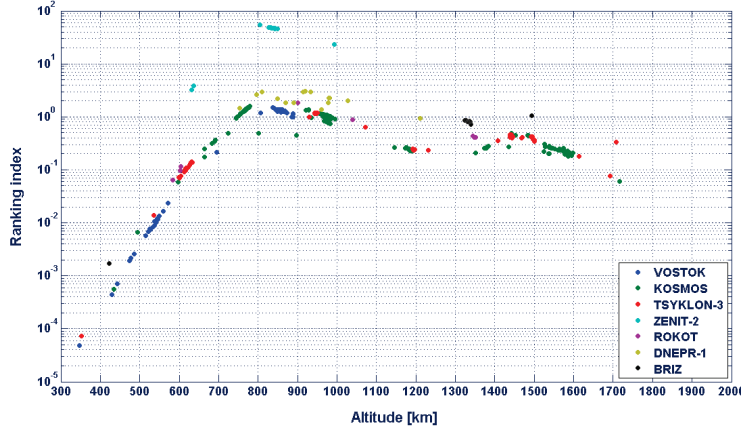


Fig. 22: Ranking of the Russian and Ukrainian rocket bodies.

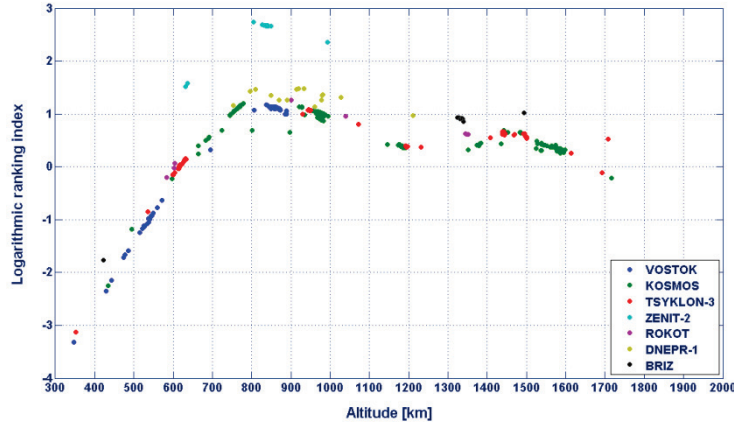


Fig. 23: Logarithmic ranking index of the Russian and Ukrainian rocket bodies.

In addition to being concentrated in relatively few and narrow inclinations bands, the most numerous rocket body families also present a significant altitude-inclination clustering (see, for example, Figures 24, 25, 26 and 27) and, in certain cases, an additional thick and quite uniform distribution in right ascension of the ascending node. This situation, particularly advantageous for multiple target removal missions [6], is especially evident for the Kosmos second stages, and will not be affected by the overall orbit evolution of the rocket bodies (Figure 24). To a lesser extent, this was also found for other rocket body families, for example the Tsylkron-3 third stages (Figure 25), the Vostok second stages (Figure 26) and the Zenit-2 second stages (Figure 27).

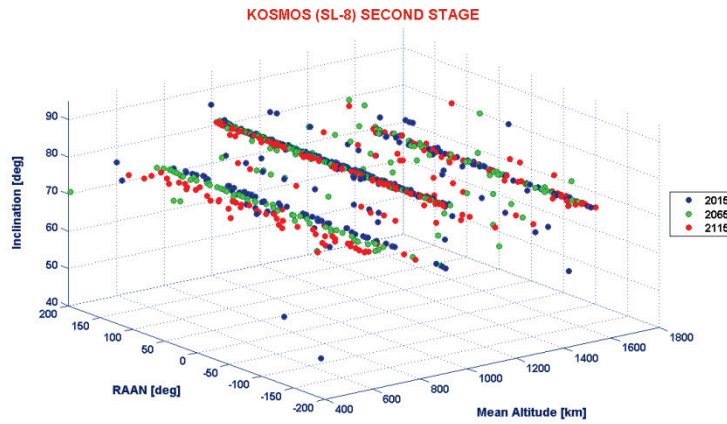


Fig. 24: Orbital distribution current status and evolution, over one century, of the Kosmos second stages. Notice the quite thick and uniform distribution in right ascension of the ascending node (RAAN) in the main altitude-inclination bands and how this overall structure is maintained during the orbital evolution.

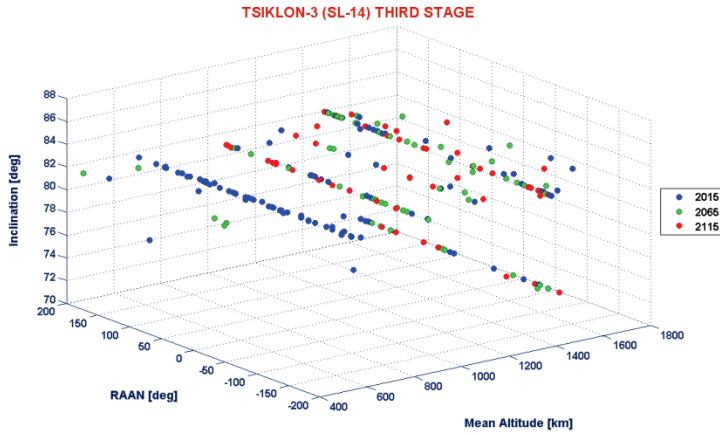


Fig. 25: Orbital distribution current status and evolution, over one century, of the Tsyklon-3 third stages.

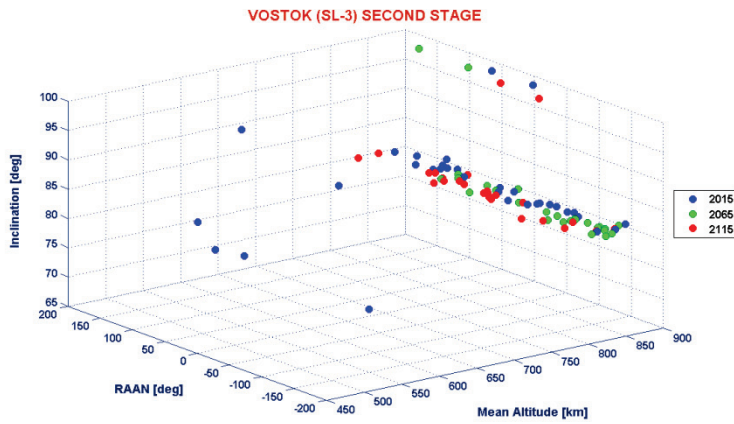


Fig. 26: Orbital distribution current status and evolution, over one century, of the Vostok second stages.

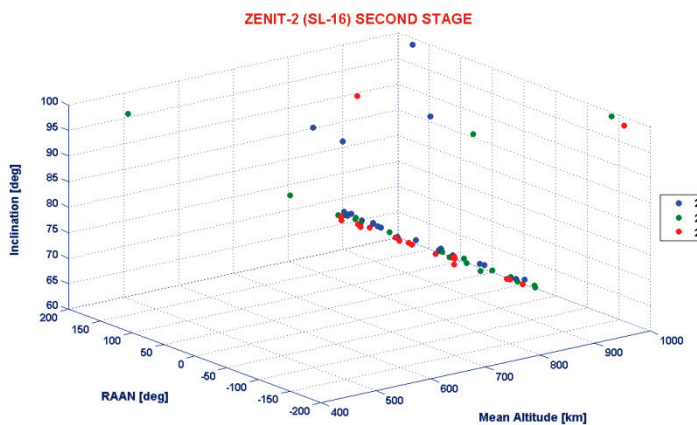


Fig. 27: Orbital distribution current status and evolution, over one century, of the Zenit-2 second stages.

The detailed results obtained for the rocket bodies associated with the American launchers are shown in Figures 28 (orbital distribution), 29 (ranking index) and 30 (logarithmic ranking index). Compared with the Russian and Ukrainian ones, the American upper stages present a larger inclination dispersion, but some groupings are discernible

as well (Figure 28). The stages for which $R_N \geq 0.1$ were found between 700 and 1800 km, and belonged to all the families (Figure 29). However, no stage was found with $R_N \geq 1$, and the six with $0.5 < R_N < 1$ were lying between 750 and 900 km.

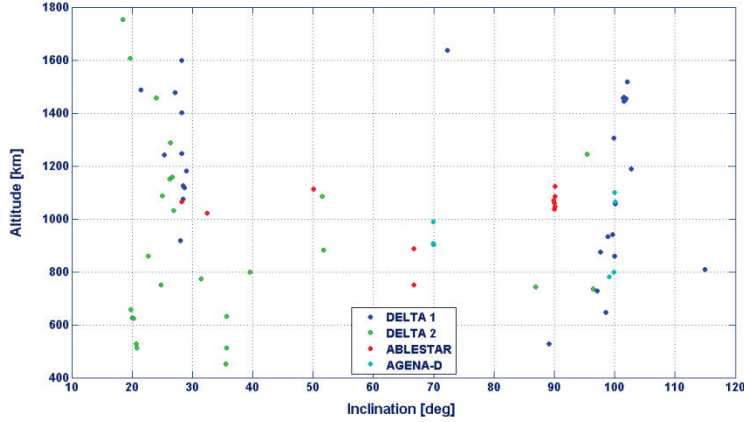


Fig. 28: Orbital distribution of the American rocket bodies.

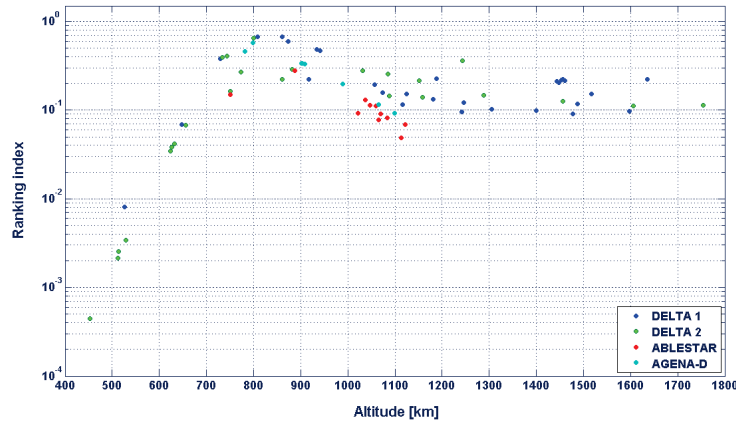


Fig. 29: Ranking of the American rocket bodies.

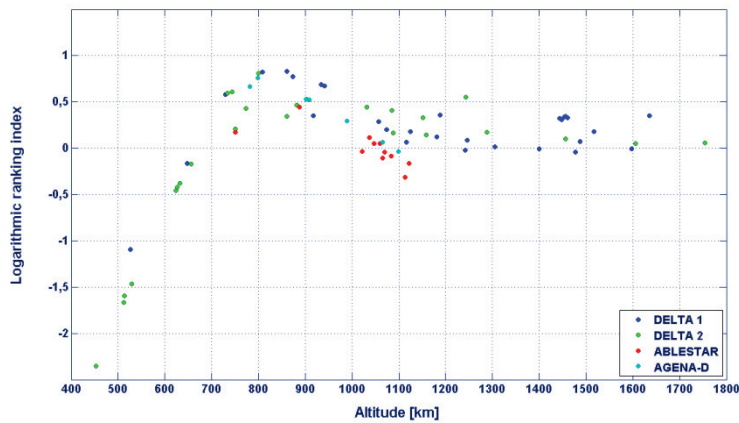


Fig. 30: Logarithmic ranking index of the American rocket bodies.

The detailed results obtained for the upper stages of the Asian and European launchers are presented in Figures 31 (orbital distribution), 32 (ranking index) and 33 (logarithmic ranking index). The only significant grouping in inclination was found in correspondence with the sun-synchronous values (Figure 31). The rocket bodies for which $R_N \geq 0.1$ were found between 500 and 1400 km, and belonged to all the families considered in the analysis (Figure 32). Those for which $R_N \geq 1$ were concentrated between 600 and 1100 km, leaving out the PSLV fourth stages. Each remaining family exhibited also some rocket bodies with $R_N \geq 2$ (Figure 20), concentrated between 650 and 900 km (Figure 32), while three CZ-2 second stages, found between 800 and 830 km, displayed a ranking index around 10.

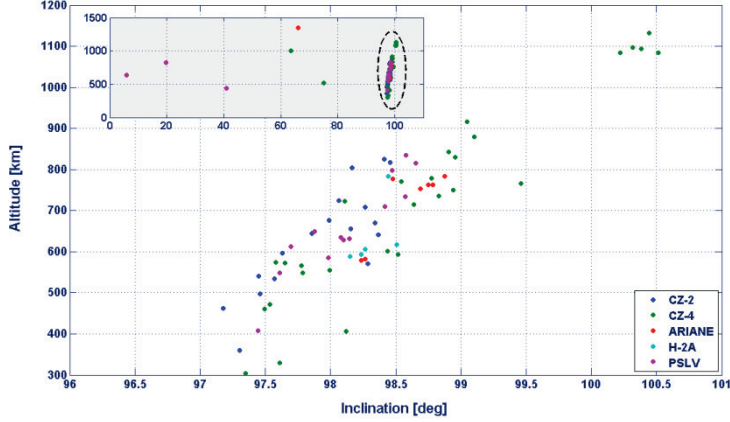


Fig. 31: Orbital distribution of the Asian and European rocket bodies.

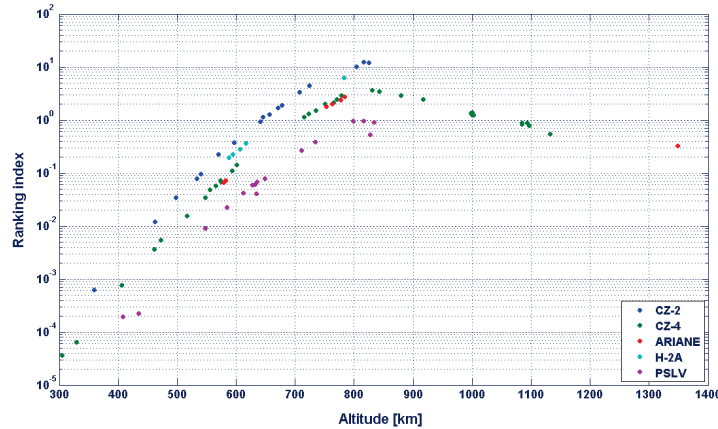


Fig. 32: Ranking of the Asian and European rocket bodies.

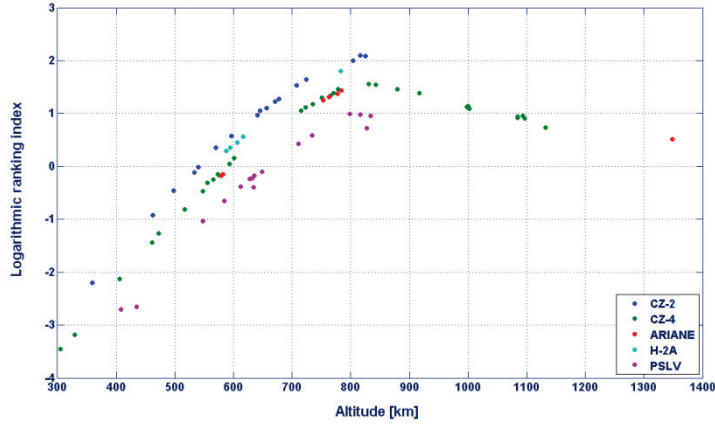


Fig. 33: Logarithmic ranking index of the Asian and European rocket bodies.

VI. CONCLUSIONS

In order to evaluate the intrinsic criticality, for the long-term evolution of the orbital debris environment, and the potential relative effectiveness of active removal, a new simplified ranking index was developed and applied to a wide set of rocket body families. They represented more than 80% of the unclassified rocket bodies in LEO and nearly 95% of the associated dry mass. The detailed results obtained for several hundred of upper stages clearly identified the most critical altitude-inclination bands and object types, to be addressed first if and when a debris remediation strategy including the active removal of abandoned mass from crowded regions were deemed necessary.

However, the usefulness of the ranking index presented and applied in this paper is not limited to debris remediation. In fact, the pre-launch application of the ranking scheme to spacecraft and rocket bodies to be disposed in orbit, after the end of the mission, would offer an additional easy to implement and apply tool for evaluating the relative advantages and disadvantages of competing disposal options. The new index may therefore benefit debris mitigation as well.

VII. REFERENCES

1. Pardini, C., Anselmo, L. Review of past on-orbit collisions among cataloged objects and examination of the catastrophic fragmentation concept, *Acta Astronautica*, 100 (2014) 30–39.
2. Anselmo, L., Pardini, C. Ranking upper stages in low Earth orbit for active removal, *Acta Astronautica*, 122 (2016) 19–27.
3. De Luca, L.T., Bernelli, F., Maggi, F., Tadini, P., Pardini, C., Anselmo, L., Grassi, M., Pavarin, D., Francesconi, A., Branz, F., Chiesa, S., Viola, N., Bonnal, C., Trushlyakov, V., Belokonov, I. Active space debris removal by hybrid engine module, *Acta Astronautica*, 91 (2013) 20–33.
4. DeLuca, L.T., Lavagna, M., Maggi, F., Tadini, P., Pardini, C., Anselmo, L., Grassi, M., Tancredi, U., Francesconi, A., Chiesa, S., Viola, N., Bonnal, C. Active removal of large massive objects by hybrid propulsion module, in: *5th European Conference for Aero-Space Sciences*, EUCASS, Paper p469, 2013.
5. De Luca, L.T., Lavagna, M., Maggi, F., Tadini, P., Pardini, C., Anselmo, L., Grassi, M., Tancredi, U., Francesconi, A., Pavarin, D., Branz, F., Chiesa, S., Viola, N. Large debris removal mission in LEO based on hybrid propulsion, *Aerotecnica Missili & Spazio, The Journal of Aerospace Science, Technology and Systems*, 93 (2014) 51–58.
6. Tadini, P., Tancredi, U., Grassi, M., Anselmo, L., Pardini, C., Francesconi, A., Branz, F., Maggi, F., Lavagna, M., DeLuca, L.T., Viola, N., Chiesa, S., Trushlyakov, V., Shimada, T. Active debris multi-removal mission concept based on hybrid propulsion, *Acta Astronautica* 103 (2014) 26–35.
7. Liou, J.-C., Johnson, N.L. A sensitivity study of the effectiveness of active debris removal in LEO, *Acta Astronautica*, 64 (2009) 236–243.
8. Liou, J.-C. An active debris removal parametric study for LEO environment remediation, *Advances in Space Research*, 47 (2011) 1865–1876.

9. Yasaka, T. Can we have an end to the debris issue?, in: *Proceedings of 62nd International Astronautical Congress*, International Astronautical Federation, Paper IAC-11-A6.5.1, 2011.
10. Utzmann, J., Oswald, M., Stabroth, S., Voigt, P., Wagner, A., Retat, I. Ranking and characterization of heavy debris for active removal, in: *Proceedings of 63rd International Astronautical Congress*, International Astronautical Federation, Paper IAC-12-A6.2.8, 2012.
11. Anselmo, L., Pardini, C. Compliance of the Italian satellites in low earth orbit with the end-of-life disposal guidelines for space debris mitigation, in: *Proceedings of 65th International Astronautical Congress*, International Astronautical Federation, Paper IAC-14-A6.4.5, 2014.
12. Radtke, J., Flegel, S.K., Roth, S., Krag, H. Deriving the spacecraft environment criticality from Monte-Carlo simulations of the space debris environment, in: *Proceedings of 65th International Astronautical Congress*, International Astronautical Federation, Paper IAC-14-A6.2.6, 2014.
13. Rossi, A., Valsecchi, G.B., Alessi, E.M. An evaluation index for the ranking of LEO objects, in: *Proceedings of 65th International Astronautical Congress*, International Astronautical Federation, Paper IAC-14-A6.2.7, 2014.
14. Anselmo, L., Pardini, C. Compliance of the Italian satellites in low earth orbit with the end-of-life disposal guidelines for space debris mitigation and ranking of their long-term criticality for the environment, *Acta Astronautica*, 114 (2015) 93–100.
15. Rossi, A., Valsecchi, G.B., Alessi, E.M. The criticality of spacecraft index, *Advances in Space Research*, 56 (2015) 449–460.
16. IADC Steering Group & Working Group 4 (Mitigation). *IADC Space Debris Mitigation Guidelines*, Document IADC-02-01 & Revision 1, Inter-Agency Space Debris Coordination Committee (IADC), 2002 & 2007.
17. Dolado-Perez, J.C., Pardini, C., Anselmo, L. Review of uncertainty sources affecting the long-term predictions of space debris evolutionary models. *Acta Astronautica*, 113 (2015) 51–65.
18. Johnson, N.L., Krisko, P.H., Liou, J.-C., Anz-Meador, P.D. NASA's new breakup model of EVOLVE 4.0, *Advances in Space Research*, 28 (2001) 1377–1384.
19. Krisko, P.H. Proper implementation of the 1998 NASA breakup model, *Orbital Debris Quarterly News*, 15–4 (2011) 4–5.
20. Pardini, C., Anselmo, L., Space debris impact risk analysis tool (SDIRAT). Report CNUCE-B4-1998-015, CNUCE Institute, CNR, Pisa, 1998.
21. Pardini, C., Anselmo, L., Assessing the risk of orbital debris impact, *Space Debris*, 1 (1999) 59–80.
22. Pardini, C., Anselmo, L., SDIRAT: Introducing a new method for orbital debris collision risk assessment, in: *Proceedings of the International Symposium on Space Dynamics*, Paper MS00/23, 2000.